Long jumps in diffusion of iridium on W(110)

Grazyna Antczak[1,2] and Gert Ehrlich[1]
[1]*Materials Research Laboratory and Department of Materials Science and Engineering, University of Illinois at Urbana-Champaign, Urbana, Illinois 61801, USA*
[2]*Institute of Experimental Physics, University of Wroclaw, Wroclaw, Poland*
(Received 24 August 2004; revised manuscript received 10 December 2004; published 22 March 2005)

Diffusion of single iridium atoms has been examined on W(110) using the field ion microscope to measure mean-square displacements as well as the distribution of displacements. The Arrhenius plot of the diffusivity, obtained from the mean-square displacements, against the reciprocal temperature gives a straight line without any indication of special behavior. From the distribution of displacements at temperatures of 331 K or lower, we find that for these conditions nearest-neighbor single jumps dominate; longer transitions are negligible. As the temperature is increased, however, the contribution of long jumps becomes more important, and at 371 K is preeminent. Both the activation energies and prefactors of the long jumps are found to be significantly higher than for nearest-neighbor transitions. The energetics of vertical and horizontal jumps are the same, unlike earlier results for the diffusion of tungsten on W(110). At elevated temperatures, the rate of nearest-neighbor jumps deviates significantly from the Arrhenius plot, suggesting that for iridium all the jump processes originate from nearest-neighbor transitions. At temperatures higher than studied here, at $T \sim 400$ K, single jumps are expected to disappear, to be replaced by longer transitions.

DOI: 10.1103/PhysRevB.71.115422 PACS number(s): 68.35.Fx, 68.35.Ja, 81.10.Aj, 81.15.Kk

I. INTRODUCTION

The usual picture of surface diffusion on a crystal is that particles jump between adjacent nearest-neighbor sites, carrying out a simple random walk. However, starting in 1979, molecular dynamics simulations by Tully *et al.*[1] and by DeLorenzi *et al.*[2,3] showed that when a surface is heated, there is a rising probability of long jumps occurring. Subsequently, Ferrando *et al.*[4] were able to obtain an expression for the distribution of jump lengths of an atom moving in a one-dimensionsl periodic potential. Their work suggested the conditions under which long jumps are expected; that is, for small values of the friction coefficient coupling the jumping atom to the heat bath. Such studies have continued, and the wealth of theoretical material has been surveyed by Ala-Nissila *et al.*[5] In contrast, there has been only little effort to probe the nature of atomic jumps in surface diffusion experimentally. A small number of investigations has appeared during the last decade which show that long jumps can take place, and indicate that as the temperature of the surface increases, longer jumps, to sites two or more spacings away, become important, as suggested by the theoretical work. This was demonstrated for diffusion of palladium on W(211),[6,7] in which movement is one-dimensional. In 1997, Linderoth *et al.*[8] used the scanning tunneling microscope to examine the distribution of Pt atoms on the reconstructed Pt(110) plane. These highly quantitative experiments were interpreted as showing both single and double jumps. However, subsequent theoretical calculations by Montalenti and Ferrando,[9] as well as by Lorensen *et al.*,[10] demonstrated that on such a reconstructed surface, rather than the atoms carrying out long jumps at the bottom of the channel, they can move to the smooth sidewalls of the diffusion channel and migrate rapidly there. Later it was shown that palladium[11] and tungsten[12] atoms execute long jumps in two-dimensional diffusion on W(110). Most recently, the rates at which long jumps occur for tungsten atoms on the W(110) surface have been examined; it has been found that long jumps have abnormally high activation energies and prefactors,[13] and that they originate from nearest-neighbor transitions.

Is this behavior confined to self-diffusion of tungsten atoms on W(110), or is it a more widespread phenomenon common to metal atoms generally? That is the specific question we address here, by carrying out an experimental examination of the behavior of iridium atoms on W(110). Iridium is, of course, a fcc metal, whereas tungsten is bcc, and the two are quite different chemically. We should therefore expect significant differences in diffusion over the surface.

Our effort will be concentrated on describing the experimental situation, whereas in previous reports on long jumps the experimental aspects of the work were only briefly considered. Here we start with a description of the equipment and routines; we then present our results for Ir diffusion on the (110) plane of tungsten, which will be compared with that of tungsten atoms and discussed in the final section.

II. EXPERIMENTAL PROCEDURES

A. Vacuum processing

For determining the movement of atoms we rely on the field ion microscope; its construction and supporting equipment have already been discussed by Reed *et al.*[14] The sample single-crystal wire of ⟨110⟩ oriented tungsten, 0.005 in. in diameter and ~0.2 in. long, obtained from FEI Company, Oregon, is spot welded onto the 0.007-in.-diameter support loop, previously aged for 24 h at ~1400 K, and is then electropolished in 2 N NaOH. Attached to the loop are two 0.005-in.-diameter potential leads, to permit measurement and control of temperature. After washing the sample and holder, mounted on a cold finger, the wire assembly is installed in the microscope. The system,

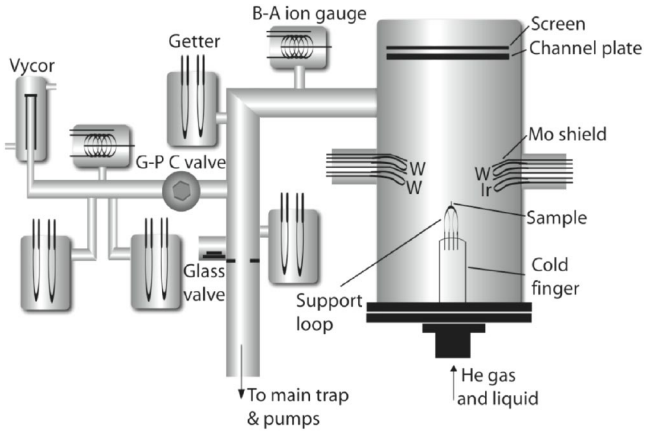

FIG. 1. Field ion microscope and vacuum system, constructed primarily of glass (Pyrex 7740). Channel plate to intensify the image has 25-μm pores and is 1.02 mm thick; the screen is made of Willemite phosphor.

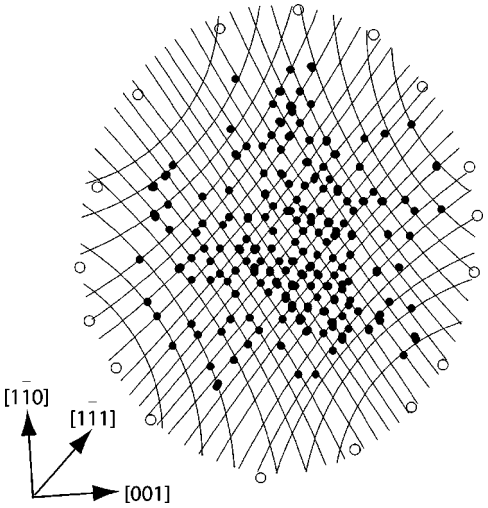

FIG. 2. Mapping of sites on W(110). Black dots show location of Ir atom after diffusion at 350 K; open circles indicate positions of substrate atoms at the plane edges.

which is evacuated by a triple-stage mercury diffusion pump backed by a mercury trap in series with a rotary pump, is illustrated in Fig. 1. It is baked out at 300 °C overnight, together with the main trap. After cooling the trap with liquid nitrogen, the oven temperature is gradually lowered, and once the temperature has reached ~175 °C, all the filaments are lit and the evaporators are heated. The ionization gauges as well as the molybdenum shields in the evaporators are cleaned by electron bombardment for ~5 h at 175 °C. Four getters in the system, made up of 0.020 in. titanium wire, are also outgassed. When the system finally reaches room temperature, heating of evaporators and getters is continued. Outgassing is then begun of the multichannel plate (obtained from Burle Electro-Optics) used to enhance the image intensity. Electrons from a nearby tungsten evaporator filament impinge on the plate with an energy of ~200 V. The sample support loop is cleaned by heating, and the tip by field evaporation at ~20 K. The tip is thereafter bombarded once by ~1-kV ions produced by electron field emission at $\sim 10^{-6}$ A in the presence of 2×10^{-4} Torr of neon, introduced through a heated Vycor tube. This ion bombardment cleans and sharpens the tip in final preparation for extended experiments. Bakeout is repeated once the pressure rises significantly. For a multichannel plate that has been exposed to the atmosphere, electron bombardment may take three weeks before the gas pressure, with all filaments hot and the shields and channel plate outgassing, is reduced to 10^{-10} Torr.

Once the system is clean, the first operation is to calibrate the tip temperature. The resistance of the tungsten support loop between the two potential leads is measured and controlled with a Kelvin double-bridge circuit, described by Reed[14] and in more detail by Koh.[15] The temperature of the support loop is then deduced from the resistance curves of Desai *et al.*;[16] standard error of the temperature measurements is ~0.5 K. Still to be determined is the temperature of the emitter tip when the support loop is heated. To do this, the rate of field evaporation of the tip with the entire system at room temperature is matched by adjusting the heating current to the support with the leads to the sample support cooled by a mixture of liquid and gaseous helium.[17] In this way, the difference between support loop and tip temperature is established; it usually amounts to ~2 K.

The first operation is to deposit iridium onto the (110) plane by heating the iridium evaporator for ~30 s at 2.3 A; this is done to check the conditions for field evaporation. Iridium atoms field evaporate readily from W(110) only when close to the edge of the surface; this is quite distinct from tungsten atoms, which field evaporate from the plane just above the voltage for good imaging. Next, the geometry of the surface is examined by depositing an Ir atom and allowing it to diffuse until much of the surface has been explored. Finally, a grid is drawn through the binding sites, as in Fig. 2, to permit mapping and determination of the plane size.

B. Imaging

Measurements of the diffusivity begin after field evaporating at least four layers and then depositing an atom on the sample surface from evaporator loops of 0.006-in.-diameter wire. After a 15 s delay, the surface is heated for a diffusion interval, and the temperature is then allowed to drop to ~20 K. Fifteen seconds later, an image is obtained in helium gas at a pressure of $\sim 10^{-4}$ Torr, and is videotaped using an RCA TC 1430R camera. The diffusion time interval is chosen so that the mean-square displacement is preferably less than five spacings. Diffusion is started with the atom in the central region of the plane, ~ ten spacings in diameter. Measurements are continued until the atom diffuses to within two spacings of the edge. That last observation is withdrawn, and the atom is allowed to migrate at 360 K until it again reaches the starting region before resuming measurements. The overall procedure is repeated 100 times, always in the absence of fields during the diffusion interval. Thereafter, the surface is cleaned by field evaporating a few layers, and another set of 100 recordings is carried out. At low temperatures, where diffusion intervals may be close to 2 min, only 100 measurements are made per day. A total of 1200 observations is

recorded, and these procedures are repeated at nine diffusion temperatures.

Atom displacements are derived by analyzing the videotapes. Twelve frames are averaged to give a good image (using modules from Data Translation, Marlboro, MA), which is examined with the NIH Image program to yield the location of the diffusing atom. With this information it is easy to evaluate the mean-square displacement both along the x and y axes; that is, along $\langle 100\rangle$ and $\langle 110\rangle$.

C. Distribution analysis

With a total of 1200 observations at one temperature, the distribution of the individual displacements can also be derived. From this distribution, information is obtained about the possible jump rates on the surface. Theoretical expressions for the distance distribution in terms of the jump rates have been derived for movement on an infinite surface.[18] In practice, however, these expressions are not really useful for analyzing measurements with the field ion microscope, as here the planes are far from infinite; typically they have a diameter of only ~22 atomic spacings along the x axis. Instead, kinetic Monte Carlo simulations are carried out on a bcc (110) plane of the same size and shape as in the experiments; the techniques have been described and tested in Ref. 19. In the simulations we deposit an atom on the central region of the plane, ~10 spacings in diameter, and allow the atom to diffuse until it comes within two spacings of the edge. The atom is then returned to the central region, and diffusion is continued. To set the rate of diffusion in the kinetic estimates, we pick trial values for the rate of single jumps, as well as for the ratio of double to single jumps, and for the difference between horizontal and vertical transitions compared to single jumps. For the waiting time between jumps and for picking the kind of jump that takes place we use the algorithm described by Reed and Ehrlich.[19] The simulated distribution so obtained is then compared with the experimentally obtained values in the simplex minimization program MINUIT, which adjusts the rates to give an improved estimate of the distribution.[20] This yields a reduced χ^2 given by

$$\chi^2 = [N_E(x,y) - N_S(x,y)]/[N\mathrm{var}(x,y)], \tag{1}$$

where $N_E(x,y)$ is the experimentally measured number of displacements at a specified site x,y, $N_S(x,y)$ is the simulated value, and N the total number of measurements at this temperature. The analysis of the experimental displacement distribution is then carried out for another set of different input parameters, and this procedure is repeated a total of 27–50 times; the best fit is determined from the most reasonable value of χ^2 obtained. The same procedure is followed separately, but allowing only single jumps, to check the possibility of fitting the distribution with nearest-neighbor jumps only.

From such a determination the contribution of long jumps to the diffusivity is immediately obvious; however, it does not give us values for the rates of long jumps at the set diffusion temperature. The steady-state temperature of the support loop is determined by the heating current through the loop. However, initially, on heating the sample, there is a finite period during which the temperature rises until the set value is reached. At the end of the diffusion interval the heating current is cut, and the temperature drops, initially quite rapidly.[21] At elevated diffusion temperatures, atom movement can take place during these temperature transients, and makes a contribution to the measured distribution. To compensate for these effects, we separately make 1200 "zero-time" measurements, in which the heating current is shut off as soon as the diffusion temperature is reached.[21] Mean-square displacements during the transients are subtracted from the values in the regular experiments. The zero-time distribution is also analyzed by Monte Carlo simulation to fit the experiments.

To determine the jump rate r at the set temperature, we subtract the number of jumps in the transient interval (obtained from fitting the displacement distribution) from that in the regular experiments in accord with[15]

$$r = (Rt - r_o t_o)/t_c, \tag{2}$$

where R is the rate and t the time in the regular experiment, r_o and t_o are the values in zero-time experiments, and t_c is the time at the diffusion temperature.

To get a feeling for the reliability of the rates, we still need to know their standard error. This we achieve as follows. From the measured rates we generate a distribution of displacements by Monte Carlo simulation. The resulting distribution is then analyzed in the usual way to derive estimates for the rates. This process of generating a distribution and then deriving rates from it is repeated at least ten times, and from this array we obtain a rough estimate of the error inherent in the rates.

III. DIFFUSION OF Ir

From the mean-square displacements of iridium on an infinite plane during a time interval t, we obtain diffusivities from

$$\langle \Delta x^2\rangle = 2D_x t = 2\Gamma_x \ell_x^2, \tag{3}$$

$$\langle \Delta y^2\rangle = 2D_y t = 2\Gamma_y \ell_y^2; \tag{4}$$

distances along the x axis are measured in terms of $a/2$, and along the y axis in terms of $\sqrt{2}a/2$, where a is the lattice constant of the substrate; Γ denotes the mean jump frequency; and ℓ an effective jump length. Our observations are, however, done on a very finite plane. We therefore carry out Monte Carlo simulations for both the regular and zero-time measurements on a plane with the same size and shape as in the experiments until simulations and experiment are in good agreement. In this way we can obtain mean-square displacements on an infinite surface. The data in Fig. 3 derived in this fashion are plotted as the logarithm of the diffusivity against $1000/T$; it gives a good Arrhenius plot without any curvature apparent at higher temperatures. The standard errors of the mean-square displacements are known from the measurements; as 1200 observations were made at each temperature, the errors are small. We note that the activation

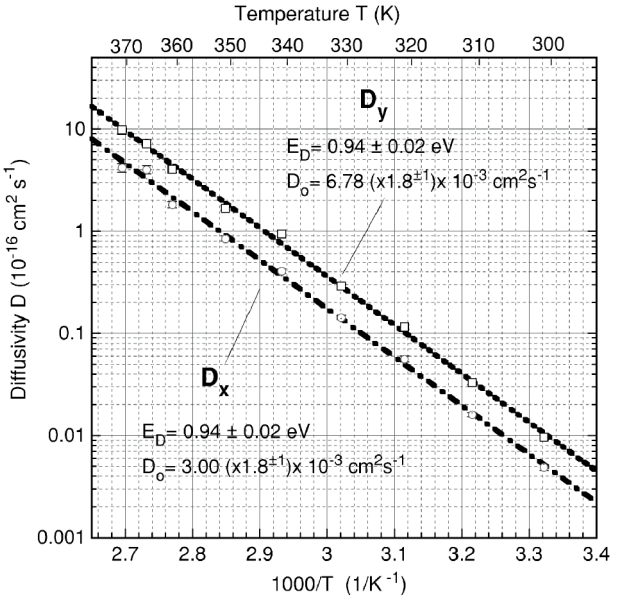

FIG. 3. Diffusivities D_x and D_y for single Ir atom on W(110) deduced from the mean-square displacement and Eqs. (3) as well as (4).

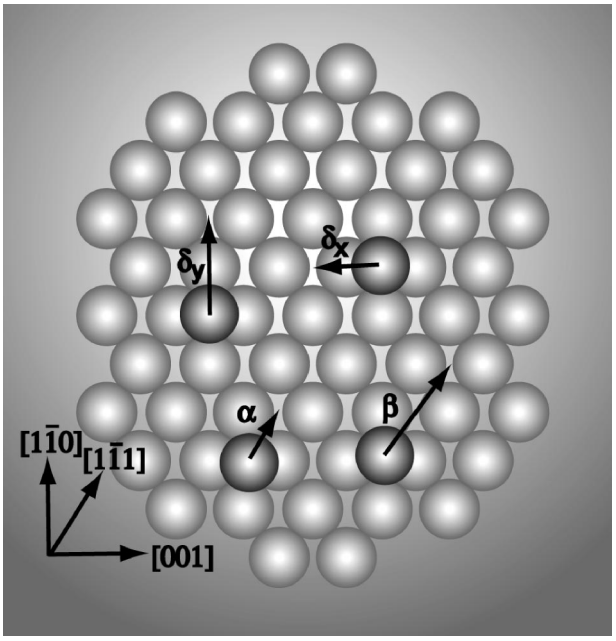

FIG. 4. Possible atom jumps on W(110) plane. In addition to nearest-neighbor transitions α and double β jumps along $[1\bar{1}1]$, we also consider horizontal δ_x and vertical δ_y jumps.

energy for diffusion along the x axis, 0.94 ± 0.02 eV, is the same as along y; the diffusion prefactor D_o along the x axis is $3.00(\times 1.8^{\pm 1}) \times 10^{-3}$ cm^2 s^{-1}, while the value along y amounts to $6.78(\times 1.8^{\pm 1}) \times 10^{-3}$ cm^2 s^{-1}. This is as expected, in view of the jump length being $\sqrt{2}$ longer along y than x. In atomic units, D_o along x and y are essentially equal. The behavior of the diffusivity therefore appears entirely normal, without giving any indication of long jumps. We also note that our results are quite close to the earlier work of Lovisa,[22] who found an activation energy of 0.97 ± 0.02 eV and a prefactor of $1.71(\times 2.3^{\pm 1}) \times 10^{-2}$ cm^2 s^{-1}.

What is actually happening in the diffusion can be derived from the distribution of displacements measured at different temperatures. Here it is a matter of deciding on the nature of the jumps to consider. The processes examined are shown in Fig. 4; these were previously derived from measurements of the diffusion of W atoms on W(110),[12] and are a good start in looking at the diffusion of iridium. Besides nearest-neighbor jumps α between adjacent sites along the close packed $\langle 111 \rangle$ direction, we also consider double jumps β along $\langle 111 \rangle$, where the adatom reaches a site two spacings from the origin. In addition, jumps δ_x along the x axis and δ_y along the y axis have previously been found important. These transitions contribute to the mean-square displacement (in atomic units) according to

$$\langle \Delta x^2 \rangle = 4\alpha t(1 + 2\delta_x/\alpha + 4\beta/\alpha), \tag{5}$$

$$\langle \Delta y^2 \rangle = 4\alpha t(1 + 2\delta_y/\alpha + 4\beta/\alpha). \tag{6}$$

The distribution of displacements found from measurements at 301 K is illustrated in Fig. 5, with all observations transposed into the first quadrant; experimental results are shown in light gray. The best fit obtained by Monte Carlo simulation is also shown, in black. At this relatively low temperature for diffusion, the best fit to the distribution reveals only single jumps to adjacent sites along $\langle 111 \rangle$; longer jumps are absent. Diffusion during temperature transients is negligible as diffusion periods are long, amounting to 110 s.

From previous observations on tungsten,[12] we know that the contribution of long transitions increases at higher temperatures. We have therefore made observations at nine dif-

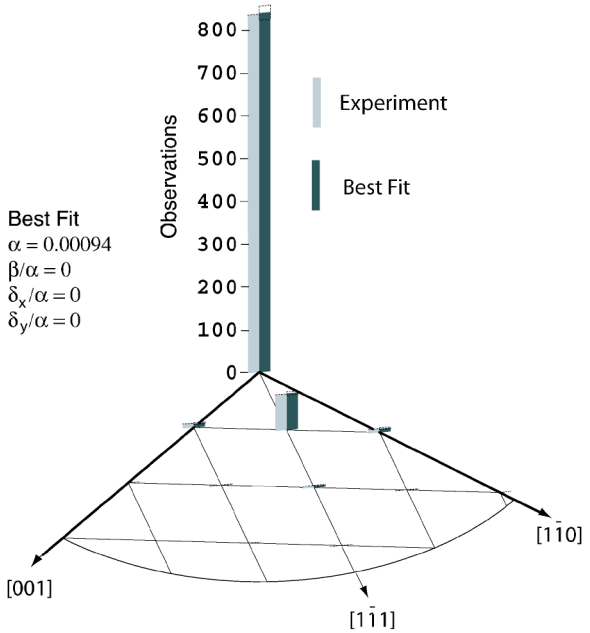

FIG. 5. Distribution of Ir displacements on W(110) for 110 s diffusion intervals at a temperature of 301 K. Experiments are given in gray, best fit in black. All measurements are shown in first quadrant. Only nearest-neighbor α jumps contribute to diffusion.

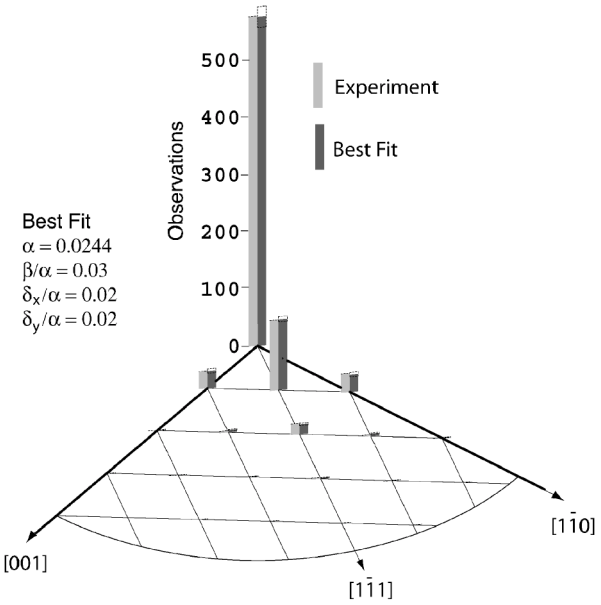

FIG. 6. Displacement distribution observed for Ir on W(110) at $T=331$ K after a 9 s diffusion interval. Experiments are drawn in gray, best fit from Monte Carlo simulations in black. The contributions of long jumps have increased above their rate at 301 K, but are still within the limit of errors.

ferent temperatures; details will only be shown for a few. Measurements for diffusion intervals of 9 s at 331 K are given in Fig. 6, which begins to reveal a very small participation of jumps other than nearest neighbors, but these are within the limits of error. Displacements at a temperature another 20 K higher, at 351 K, are shown in Fig. 7. Here it is clear that the contribution of long jumps has become nonnegligible. The ratio of double to single jumps (β/α) amounts to 0.06; for horizontal as well as for vertical jumps the ratio to singles is 0.10. Zero-time contributions during the temperature transients for this diffusion temperature have increased, and are also shown.

These trends continue as the diffusion temperature is raised. In Figs. 8 and 9 we show the results for regular measurements at $T=366$ K and 371 K, together with the distributions from zero-time determinations. At the highest tem-

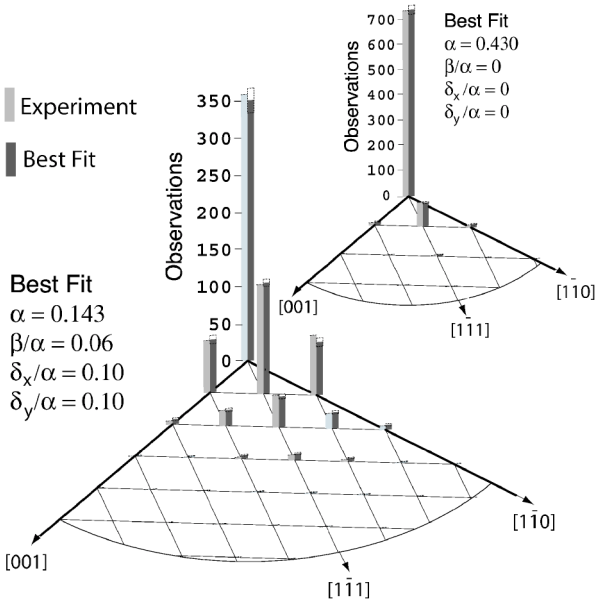

FIG. 7. Distribution of Ir displacements on W(110) after 3 s at 351 K. At this temperature long jumps have become significant. The distribution in zero-time measurements, which is now important, is shown at the upper right.

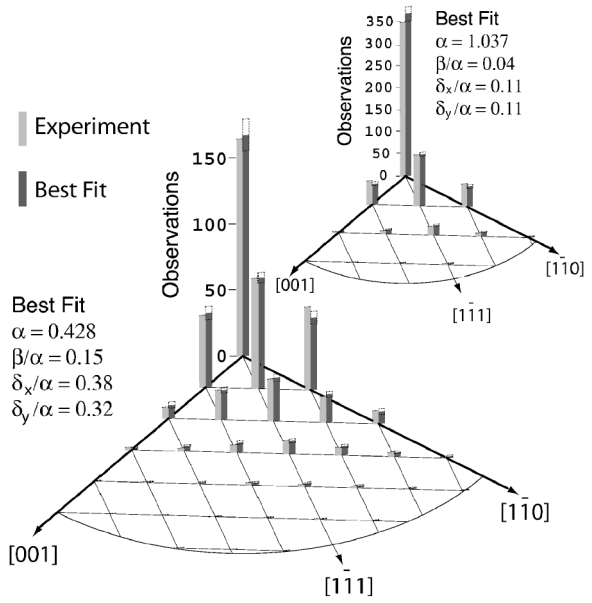

FIG. 8. Displacements during diffusion of Ir on W(110) during a 1 s interval at 366 K. All long jumps are contributing significantly at this temperature. Zero-time distribution of displacements for this diffusion temperature is at the upper right.

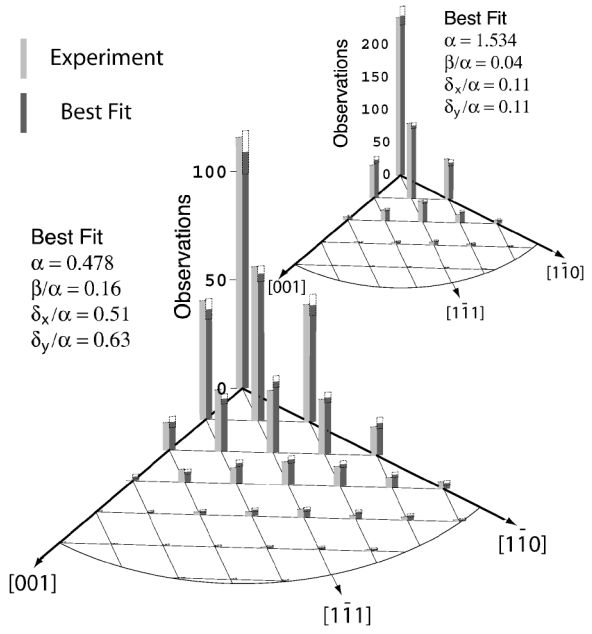

FIG. 9. Distribution of displacements for Ir at the highest diffusion temperature of 371 K. Diffusion interval is 1 s. Long jumps are now dominant in diffusion. Zero-time distribution is given at the upper right.

TABLE I. Rate ratios for Ir on W(110).

	Regular				Final			
T (K)	α	β/α	δ_x/α	δ_y/α	α	β/α	δ_x/α	δ_y/α
301	0.00094	0	0	0	0.00094	0	0	0
311	0.00286	0	0.0634	0.0634	0.00288	0	0.0635	0.0635
321	0.00976	0.0283	0.0311	0.0311	0.00988	0.0328	0.0311	0.0311
331	0.0244	0.0337	0.0241	0.0241	0.0252	0.0336	0.0241	0.0241
341	0.0714	0.0435	0.0610	0.146	0.0646	0.0506	0.0711	0.170
351	0.143	0.0583	0.0996	0.0996	0.111	0.0834	0.143	0.143
361	0.366	0.0833	0.0137	0.0684	0.237	0.140	0.0264	0.101
366	0.428	0.146	0.378	0.322	0.168	0.438	1.090	0.886
371	0.478	0.161	0.514	0.625	0.0250	3.399	11.26	14.27

perature at which we have made observations, 371 K, the contributions of long jumps are very large. The ratio of double to single jumps in the regular experiments is 0.16, of horizontal to single jumps 0.51, and of vertical to single jumps 0.63. It should also be noted that the zero-time distribution now also requires longer transitions to achieve a reasonable fit. For these measurements at a diffusion temperature of 371 K, we find $\beta/\alpha=0.04$ and δ_x/α as well as δ_y/α is 0.11.

Using the zero-time experiments we have corrected the regular measurements. From the distributions we obtain the ratios of long jumps to nearest-neighbor transitions during temperature transients. These zero-time experiments are dominated by nearest-neighbor jumps, and their contribution to the final values increases with rising diffusion temperature. Therefore, when corrections are made using Eq. (2) the effect is to further lower the nearest-neighbor α rate. The ratios of long to single jumps for all our measurements are listed in Table I. It is evident that the zero-time corrections have a very significant effect at higher temperatures.

The behavior of the different jumps is most clearly shown in Arrhenius plots, which reveal the importance of long jumps in the surface diffusion of iridium on W(110). The most interesting of these is the plot for nearest-neighbor jumps α in Fig. 10. What is quite clear is that at low temperatures, the rate α behaves normally. As the temperature is increased, however, the actual jump rate departs from a straight Arrhenius plot of the logarithm for the rate versus $1000/T$; it goes through a maximum, and then diminishes. As shown in Figs. 11–13, the rates for other jumps do not behave this way; they all have straight Arrhenius plots over the entire temperature range from 301 to 371 K.

IV. COMPARISON AND DISCUSSION

The activation energies and prefactors derived from our experiments for the different kinds of jumps are listed in

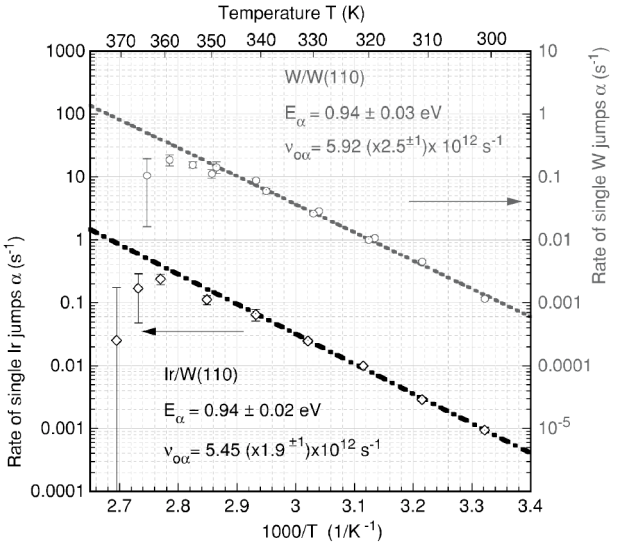

FIG. 10. Temperature dependence of the rate of single α jumps for Ir adatom and also W on W(110) (Ref. 13). Straight lines are fitted to data at or below 340 K, where long jumps are not yet important. At higher temperatures, jump rate α deviates significantly from Arrhenius plot.

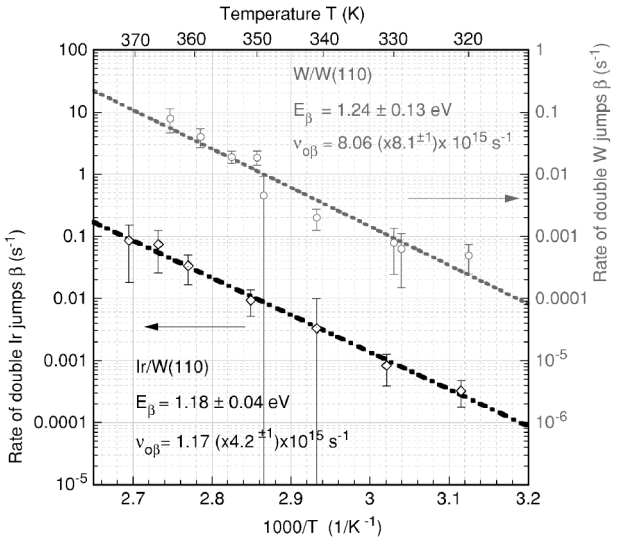

FIG. 11. Rates of double β jumps for Ir and W on W(110) as a function of $1000/T$. Straight lines fit experimental data over entire temperature range. Tungsten data from Ref. 13.

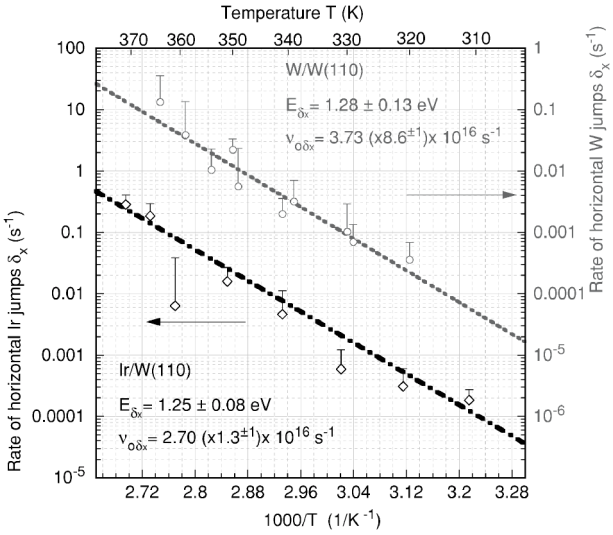

FIG. 12. Rates for horizontal δ_x jumps of Ir and W atoms on W(110), the latter from Ref. 13. The two rates are essentially the same, and are well described by a straight line for all the temperatures. Only upper error bars are shown.

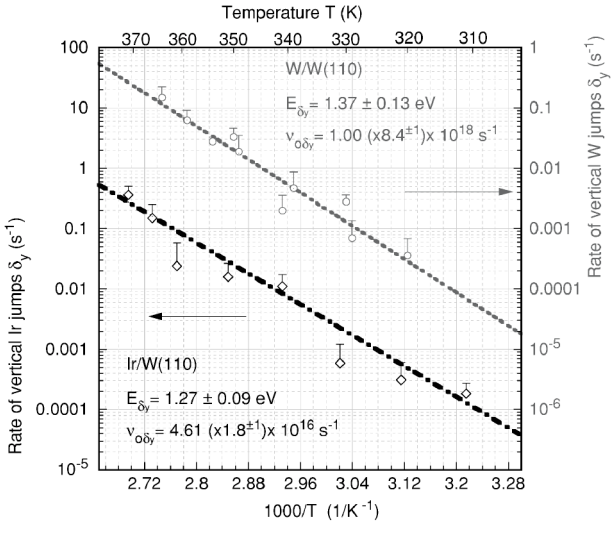

FIG. 13. Vertical δ_y jump rates for Ir as well as W on W(110). The two rates differ significantly. For Ir, the vertical jump rate is the same as the horizontal. Only upper error bars are shown. Tungsten data are from Ref. 13.

Table II. It is clear that at higher temperatures long jumps play a major role. At 371 K, the rate of double jumps β is three times that of single jumps, horizontal δ_y transitions are 11 times higher, and vertical jumps δ_y are 14 times higher. What is evident is that the barriers to long jumps are significantly larger than for nearest-neighbor transitions, and the same is true of the prefactors. This is in accord with the appearance of long jumps only at higher temperatures. The activation energy for double jumps is 25% higher than for for singles, the barriers for horizontal and vertical jumps are the same and $\sim 1/3$ higher than for singles.

It must be noted that even though our measurements are extensive, we have covered only a small range of temperatures, when considering the fact that the melting point of tungsten is 3695 K, 10 times higher than our highest diffusion temperature. At more elevated temperatures than covered here, at $T \sim 400$ K, the long jumps we have invoked, together with other long transitions, can be expected to dominate the transport of atoms over the surface. Single atom jumps will make entirely negligible contributions to the diffusivity. Much the same can be said about the diffusion of tungsten atoms on W(110), which we previously examined.[12,13]

Comparison of the behavior of iridium atoms with that of tungsten is worthwhile, as, surprisingly enough, there are similarities. The previously measured activation energies and prefactors for diffusion processes of tungsten[13] are also given in Table II. The rates of horizontal δ_x jumps in Fig. 12 and vertical δ_y jumps in Fig. 13 are essentially the same for iridium. For tungsten, shown in the same graphs, they are rather different, with the barrier and prefactor for δ_y significantly larger than for δ_x. The chemical nature of the diffusing atom apparently does play a role in influencing the jump processes. This happens even though the overall diffusivity of iridium and tungsten on W(110) is quite the same, despite the marked difference in the bulk properties of the two materials: the heat of vaporization is 6.24 eV for iridium, but 8.51 eV for tungsten.

One possible rationalization for this equality is that diffusion on W(110) occurs via an exchange mechanism,[23] in which movement occurs by the iridium deposited on the surface exchanging with a neighboring substrate tungsten atom, which moves to the surface and perpetuates motion. To check this possibility we measured the conditions for evaporation after every second measurement cycle. From these measurements, it is clear that at the end of an experiment the

TABLE II. Rate parameters on W(110).

	Ir/W(100)		W/W(110)[a]	
Rate	Activation energy E (eV)	Frequency prefactor ν_o (s^{-1})	Activation energy E (eV)	Frequency prefactor ν_o (s^{-1})
α	0.94±0.02	$5.45(\times 1.9^{\pm 1}) \times 10^{12}$	0.94±0.03	$5.92(\times 2.5^{\pm 1}) \times 10^{12}$
β	1.18±0.04	$1.17(\times 4.2^{\pm 1}) \times 10^{15}$	1.24±0.13	$8.06(\times 8.1^{\pm 1}) \times 10^{15}$
δ_x	1.25±0.08	$2.70(\times 1.3^{\pm 1}) \times 10^{16}$	1.28±0.13	$3.73(\times 8.6^{\pm 1}) \times 10^{16}$
δ_y	1.27±0.09	$4.61(\times 1.8^{\pm 1}) \times 10^{16}$	1.37±0.13	$1.00(\times 8.4^{\pm 1}) \times 10^{18}$

[a]From Ref. 6.

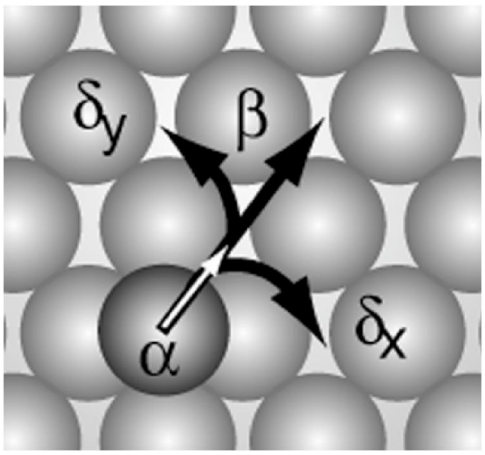

FIG. 14. Processes responsible for long jumps on W(110). Basic event is transition α to a nearest-neighbor site. At higher temperatures, this jump may continue to a site two spacings away, a β jump, or deviate to the right (δ_x) or left (δ_y).

atom diffusing on the surface is iridium and not tungsten; this rules out exchange occurring during diffusion.

The single jump rate α for iridium is compared in Fig. 10 with values measured for tungsten.[13] This rate behaves in much the same way for both atoms, increasing at first but eventually going through a maximum and then decreasing as the temperature is increased. The explanation previously offered for W also seems applicable to Ir atoms. The long jumps of Ir appear to stem from the basic jump process on the surface, which is the movement of an atom to a nearest-neighbor position. At higher temperatures, the atom does not always de-excite at the neighboring site, however. It can continue to a site along $\langle 111 \rangle$ two spacings from the start, or else it can deviate to a neighbor at the right or left, as suggested in Fig. 14; that is, the atom can make horizontal δ_x jumps or vertical δ_y jumps. Every time a long jump occurs, the rate of single jumps to a nearest-neighbor site is diminished, so that at more elevated temperatures where long jumps become more important, the rate α deviates ever more strongly from the linear Arrhenius plot, as shown in Fig. 10. At temperatures around ~400 K, not accessible to our measurements, the same type of process can be expected to occur with β double jumps. The net effect may therefore be a diminution of the contributions of β jumps, similar to what we have found for nearest-neighbor α jumps in our temperature range. In this range of much higher temperatures, even longer jumps can be expected.

A question still remains about the factors responsible for vertical and horizontal transitions on W(110). Our measurements establish the existence of such transitions, but not their detailed paths over the surface. It is the interactions between the jumping atom and the lattice that dictate how a jump proceeds. As is clear from the difference in horizontal and vertical jump rates for Ir and for W, these interactions are different for the two systems. The interactions between adatoms and the surface are, of course, also crucial in determining the conditions under which long jumps occur.[24,25] At the moment, however, there is no simple relation between the frictional coefficient parameter, usually invoked to account

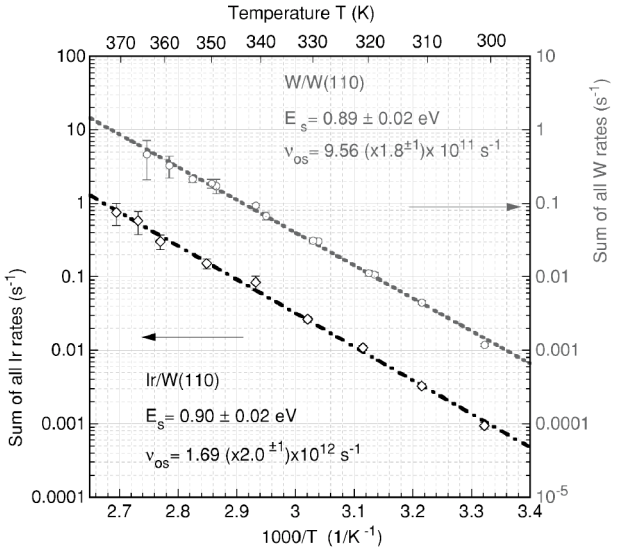

FIG. 15. Sum of all jump rates in diffusion for Ir and also W on W(110) (Ref. 13). A straight line covers the data points over the entire temperature range.

for long jumps, and the physical properties of the lattice.

The question now arises as to why the activation energies and prefactors of the long jumps are so much higher than for nearest-neighbor transitions. We can write the rate r_i of a long jump i as given by the product of the basic jump rate $R = \nu \exp(-E/kT)$, multiplied by the probability p_i of a deviation occurring, giving

$$r_i = Rp_i. \tag{7}$$

The deviation probability can be written as $p_i = \nu_i \exp(-E_i/kT)$, so that we finally have

$$r_i = \nu\nu_i \exp[-(E + E_i)kT]. \tag{8}$$

The prefactor for the long jump rate appears as a product, and is therefore very likely larger than for single jumps; the overall activation energy is the sum of the barrier to the basic jump plus that of the deviation, and will therefore also be on the large side.

If this picture is correct, and long jumps have their origin in nearest-neighbor transitions, then the sum of all jump rates should be equal to that of single α jumps extrapolated from lower temperatures. That is indeed the case both for Ir and W, as is apparent in Fig. 15. This appears to be the behavior typical of diffusion on tungsten (110). Is such behavior general for other surfaces as well? That is something that will have to be examined in the future.

ACKNOWLEDGMENTS

This work was supported by the Department of Energy under Grant No. DEFG02-91ER45439 to the Materials Research Laboratory, and by the Petroleum Research Fund under Grant SCS PRF No. 36919-ACP. We want to thank W. I. Lawrence for his help with our equipment.

[1] J. C. Tully, G. H. Gilmer, and M. Shugard, J. Chem. Phys. **71**, 1630 (1979).
[2] G. DeLorenzi, G. Jacucci, and V. Pontikis, in Proc. ICSS-4 and ECOSS-3, edited by D. A. Degras and M. Costa, Cannes, 1980, Vol. 1, p. 54.
[3] G. DeLorenzi, G. Jacucci, and V. Pontikis, Surf. Sci. **116**, 391 (1982).
[4] R. Ferrando, R. Spadacini, and G. E. Tommei, Phys. Rev. E **48**, 2437 (1993).
[5] T. Ala-Nissila, R. Ferrando, and S. C. Ying, Adv. Phys. **51**, 949 (2002).
[6] D. C. Senft and G. Ehrlich, Phys. Rev. Lett. **74**, 294 (1995).
[7] D. C. Senft, Appl. Surf. Sci. **94/95**, 231 (1996).
[8] T. R. Linderoth, S. Horch, E. Laegsgaard, I. Stensgaard, and F. Besen-bacher, Phys. Rev. Lett. **78**, 4978 (1997).
[9] F. Montalenti and R. Ferrando, Phys. Rev. B **58**, 3617 (1998).
[10] H. T. Lorensen, J. K. Norskov, and K. W. Jacobsen, Phys. Rev. B **60**, R5149 (1999).
[11] S.-M. Oh, S. J. Koh, K. Kyuno, and G. Ehrlich, Phys. Rev. Lett. **88**, 236102 (2002).
[12] S.-M. Oh, K. Kyuno, S. J. Koh, and G. Ehrlich, Phys. Rev. B **66**, 233406 (2002).
[13] G. Antczak and G. Ehrlich, Phys. Rev. Lett. **92**, 166105 (2004).
[14] D. A. Reed and G. Ehrlich, Surf. Sci. **151**, 143 (1985).
[15] S. J. Koh, Ph.D. thesis, University of Illinois at Urbana-Champaign, Urbana-Champaign, 1998.
[16] P. D. Desai, T. K. Chu, H. M. James, and C. Y. Ho, J. Phys. Chem. Ref. Data **13**, 1069 (1984).
[17] S. C. Wang and G. Ehrlich, Surf. Sci. **206**, 451 (1988).
[18] J. D. Wrigley, M. E. Twigg, and G. Ehrlich, J. Chem. Phys. **93**, 2885 (1990).
[19] D. A. Reed and G. Ehrlich, Surf. Sci. **105**, 603 (1981).
[20] F. James, CERN Program Library Long Writeup D506, 1998 (unpublished).
[21] M. F. Lovisa and G. Ehrlich, Surf. Sci. **246**, 43 (1991).
[22] M. Lovisa and G. Ehrlich, J. Phys. (France) **50**, C8 (1989).
[23] R. Gomer, Rep. Prog. Phys. **53**, 917 (1990).
[24] L. Y. Chen and S. C. Ying, Phys. Rev. B **49**, 13 838 (1994).
[25] L. Y. Chen, M. R. Baldan, and S. C. Ying, Phys. Rev. B **54**, 8856 (1996).